



## NRC Publications Archive Archives des publications du CNRC

### **HVOF-Sprayed Al<sub>2</sub>O<sub>3</sub>-TiO<sub>2</sub> Coatings Using Hybrid (Nano+Submicron) Powders: an Enhanced Wear Performance** Lima, R. S.; Moreau, C.; Marple, B. R.

This publication could be one of several versions: author's original, accepted manuscript or the publisher's version. /  
La version de cette publication peut être l'une des suivantes : la version prépublication de l'auteur, la version acceptée du manuscrit ou la version de l'éditeur.

#### **Publisher's version / Version de l'éditeur:**

*Proceedings of the International Thermal Spray Conference and Exposition, 2007., 2007-05-16*

#### **NRC Publications Record / Notice d'Archives des publications de CNRC:**

<https://nrc-publications.canada.ca/eng/view/object/?id=e1bcc5e7-34c3-463d-952a-81d8d1108d5c>  
<https://publications-cnrc.canada.ca/fra/voir/objet/?id=e1bcc5e7-34c3-463d-952a-81d8d1108d5d>

Access and use of this website and the material on it are subject to the Terms and Conditions set forth at  
<https://nrc-publications.canada.ca/eng/copyright>  
READ THESE TERMS AND CONDITIONS CAREFULLY BEFORE USING THIS WEBSITE.

L'accès à ce site Web et l'utilisation de son contenu sont assujettis aux conditions présentées dans le site  
<https://publications-cnrc.canada.ca/fra/droits>  
LISEZ CES CONDITIONS ATTENTIVEMENT AVANT D'UTILISER CE SITE WEB.

**Questions?** Contact the NRC Publications Archive team at  
PublicationsArchive-ArchivesPublications@nrc-cnrc.gc.ca. If you wish to email the authors directly, please see the first page of the publication for their contact information.

**Vous avez des questions?** Nous pouvons vous aider. Pour communiquer directement avec un auteur, consultez la première page de la revue dans laquelle son article a été publié afin de trouver ses coordonnées. Si vous n'arrivez pas à les repérer, communiquez avec nous à PublicationsArchive-ArchivesPublications@nrc-cnrc.gc.ca.



# HVOF-Sprayed Al<sub>2</sub>O<sub>3</sub>-TiO<sub>2</sub> Coatings Using Hybrid (Nano+Submicron) Powders: an Enhanced Wear Performance

R. S. Lima, C. Moreau, B. R. Marple  
National Research Council of Canada, Boucherville, QC, Canada

IMI 2006-115157-g  
CNRC 48956

## Abstract

In previous studies, it has been demonstrated that nanostructured Al<sub>2</sub>O<sub>3</sub>-13wt%TiO<sub>2</sub> coatings deposited via air plasma spray (APS) exhibit higher wear resistance when compared to that of conventional coatings. This study aimed to verify if HVOF-sprayed Al<sub>2</sub>O<sub>3</sub>-13wt%TiO<sub>2</sub> coatings produced using hybrid (nano+submicron) powders could improve even further the already recognized good wear properties of the APS nanostructured coatings. According to the abrasion test results (ASTM G 64), there was an improvement in wear performance by a factor of 8 for the HVOF-sprayed hybrid coating as compared to the best performing APS conventional coating. When comparing both hybrid and conventional HVOF-sprayed coatings, there was an improvement in wear performance by a factor of 4 when using the hybrid material. The results show a significant anti-wear improvement provided by the hybrid material. Scanning electron microscopy (SEM) at low/high magnifications showed the distinctive microstructure of the HVOF-sprayed hybrid coating, which helps to explain its excellent wear performance.

## Introduction

### Improved Wear Resistance of Air Plasma Sprayed Nanostructured Al<sub>2</sub>O<sub>3</sub>-13wt%TiO<sub>2</sub> Coatings

It has been demonstrated by other researchers that nanostructured Al<sub>2</sub>O<sub>3</sub>-13wt%TiO<sub>2</sub> coatings, made from nanostructured agglomerated powders and deposited via air plasma spray (APS), exhibit an enhanced wear performance when compared to conventional Al<sub>2</sub>O<sub>3</sub>-13wt%TiO<sub>2</sub> coatings (made from clad powders) also deposited via APS [1, 2]. Surprisingly, it was observed that the nanostructured coatings were not harder than the conventional ones; however, the nanostructured coatings exhibited enhanced crack propagation resistance, i.e., they were tougher. This higher toughness of the nanostructured coatings is considered as the main responsible characteristic for their good wear performance levels.

### Enhanced Wear Performance of HVOF-Sprayed Nanostructured Ceramic Oxide Coatings

Conventional (fused and crushed) and nanostructured TiO<sub>2</sub> powders were sprayed by APS and HVOF. The abrasion wear of these coatings was tested. From the APS conventional to the HVOF-sprayed conventional TiO<sub>2</sub> coatings there was a reduction in the volume loss of 44%. However, from the APS conventional to the HVOF-sprayed nanostructured TiO<sub>2</sub> coatings there was a reduction in the volume loss of ~60% for the same wear testing conditions [3].

These results demonstrate that the wear performance of HVOF-sprayed nanostructured ceramics seems to be unmatched by that of APS conventional ceramics. Consequently, as Al<sub>2</sub>O<sub>3</sub>-13wt% TiO<sub>2</sub> is considered a stronger material when compared to TiO<sub>2</sub>, it is a logical step to apply the same concept to Al<sub>2</sub>O<sub>3</sub>-13wt% TiO<sub>2</sub>.

## Experimental Procedure

### Powders

One nanostructured (as designated by the manufacturer) and two conventional Al<sub>2</sub>O<sub>3</sub>-13wt% TiO<sub>2</sub> feedstock powders were employed in this work. The "nanostructured" Al<sub>2</sub>O<sub>3</sub>-13wt% TiO<sub>2</sub> feedstock (Nanox S2613S, Inframat Corp., Farmington, CT, USA) was made by spray-drying. This feedstock was sieved (air classifier) to separate the particles into two groups, fine cut for HVOF spraying and large cut for air plasma spraying. The first conventional feedstock Al<sub>2</sub>O<sub>3</sub>-13wt% TiO<sub>2</sub> (Metco 130, Sulzer Metco, Westbury, NY, USA) was made via the cladding of fused and crushed Al<sub>2</sub>O<sub>3</sub> particles by a thin layer of submicron TiO<sub>2</sub> particles. The second Al<sub>2</sub>O<sub>3</sub>-13wt% TiO<sub>2</sub> feedstock (Amperit 744.0, H. C. Starck, Goslar, Germany) is a blend of Al<sub>2</sub>O<sub>3</sub> and TiO<sub>2</sub> particles, and it was also sieved (air classifier) in order to obtain a fine particle cut for HVOF spraying. The particle size distribution of the powders was determined using a laser diffraction particle size

analyzer (Beckman Coulter LS 13320, Beckman Coulter, Miami, FL, USA).

### Torches and Thermal Spraying

The combination of powders, processes and torches employed in this study can be found in Table 1.

*Table 1: The torches, processes and powders.*

Powder	Process	Torch
Metco 130	APS	F4-MB* / SG100**
Nanox S2613S (APS cut)	APS	F4-MB*
Amperit 744.0 (HVOF cut)	HVOF	DJ2700-hybrid*
Nanox S2613S (HVOF cut)	HVOF	DJ2700-hybrid*

\* Sulzer Metco, Westbury, NY, USA

\*\* Praxair, Concord, NH, USA

For the APS coatings (Ar/H<sub>2</sub> plasma), various spray parameters were initially tested by monitoring the particle temperature (T) and velocity (V) using a diagnostic tool based on pyrometric and time-of-flight measurements (DPV 2000, Tecnar Automation, Saint Bruno, QC, Canada). The parameter sets that produced a wide range of T & V values were selected for coating production. A total of three “nanostructured” and four conventional Al<sub>2</sub>O<sub>3</sub>-13wt% TiO<sub>2</sub> coatings were produced via APS. For HVOF spraying, various spray parameters were also initially tested by monitoring particle T & V by using the DPV 2000. The parameter set that produced the highest average particle temperature for the two feedstock powders was selected for coating production, i.e., two coatings (one “nanostructured” and one conventional) were produced via HVOF spraying. For each spraying case, a total of 5000 particles were measured at the centerline of the spray jet where the particle flow density was the highest. The particle detector was placed at the same spray distance as used when depositing the coatings.

The coatings were deposited on low-carbon steel substrates (width: 2.54 cm; length: 7.62 cm; thickness: 1.27 cm) that had been grit-blasted with alumina to roughen the surface before spraying. During the spraying process, a cooling system consisting of air jets was applied to reduce the coating temperature. The coating temperature was monitored during spraying using an optical pyrometer (focused at the coating surface). The maximum temperatures during the process were ~280°C and ~180°C, respectively, for the HVOF-sprayed and air plasma sprayed coatings. The typical coating thickness was 450-550 µm.

### Nanostructure, Microstructure and Porosity

The nanostructural and microstructural features of the powders were analyzed via scanning electron microscopy (SEM). The overall coating microstructure and porosity were also analyzed

via SEM and image analysis. A total of ten images (500 X) per coating were analyzed to determine porosity levels.

### Microhardness and Crack Propagation Resistance

Vickers microhardness measurements were performed under a 300 g load for 15 s on the cross-sections of the coatings. A total of 10 microhardness measurements were carried out for each coating.

The crack propagation resistance was determined by indenting the coating cross-sections with a Vickers indenter at a 5 kg load for 15 seconds, with the indenter aligned such that one of its diagonals would be parallel to the substrate surface. The total length (tip-to-tip) of the major crack (2c) parallel to the substrate surface that originated at or near the corners of the Vickers indentation impression was measured. Based on the indentation load (P) and 2c, the crack propagation resistance was calculated according to the relation between load and crack length  $P/c^{3/2}$ , where P is in Newtons and c is in meters [4]. A total of 5 indentations were carried out for each coating.

### Abrasion Wear Resistance

The abrasion resistance of the coatings was tested based on the standard ASTM G65-00 (procedure D, modified) [5], which is also known as the dry sand/rubber wheel test. In this test a stationary coated sample was pressed against a rotating rubber-coated wheel (diameter 228.6 mm; 200 rpm) with a force of 45 N. Silica sand (212-300 µm) was fed (300-400 g/min) between the coating and the rubber wheel until the wheel traveled over the equivalent linear distance of 1436 m. Prior to being tested, the surfaces of the coatings were prepared by grinding with diamond wheels to produce a leveled surface and a surface finish of  $R_a \sim 0.2$  µm. Two samples were tested for each coating produced in this study. The volume of the material abraded away during the wear test was measured via optical profilometry.

## **Results and Discussion**

### Feedstock Powders

The particle size cut of the powders is shown in Table 2. It can be observed that the powder particles employed for APS were larger than those employed for HVOF. It was previously shown that a particle size distribution from 5 to 20 µm is approximately the optimal cut for HVOF spraying of ceramics [6]. It is important to point out that the two groups of powders designated to be sprayed via HVOF and APS exhibited, in general, similar particle size cuts. This characteristic is important in order to observe real effects of the feedstock structure (and not feedstock size) on the coating microstructure and properties. The SEM powder pictures can be found in Figs. 1-2. It is important to point out that these pictures (at low magnification) were taken using backscattered electrons (BSE).

Table 2: Particle size distribution (in volume).

Powder	d <sub>10</sub> (μm)	d <sub>50</sub> (μm)	d <sub>90</sub> (μm)
Metco 130	24	36	53
Nanox S2613S (APS cut)	14	39	62
Amperit 744.0 (HVOF cut)	6	10	16
Nanox S2613S (HVOF cut)	2	15	24

Therefore they can be used to contrast elements based on differences in atomic numbers (e.g., Al: 13 and Ti: 22). The lower atomic number elements will appear darker than the heavier ones in the SEM picture. This phenomenon is caused because the backscattered electron yield is proportional to the atomic number of the material. Figure 1 shows the SEM picture of the Al<sub>2</sub>O<sub>3</sub>-13wt% TiO<sub>2</sub> feedstock powder Amperit 744.0. It is possible to confirm that this feedstock is blended, i.e., formed by the mixture of fused and crushed Al<sub>2</sub>O<sub>3</sub> and TiO<sub>2</sub> particles.

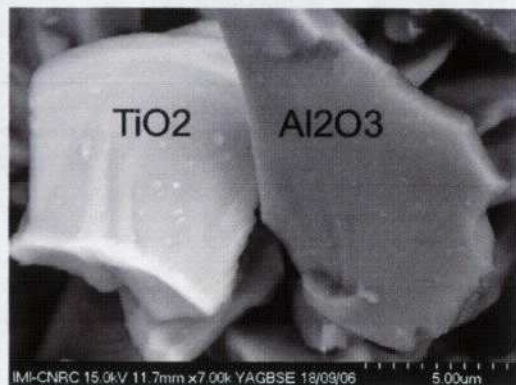


Figure 1: SEM picture (BSE) of the Al<sub>2</sub>O<sub>3</sub>-13wt% TiO<sub>2</sub> powder Amperit 744.0.

Figure 2 shows the “nanostructured” Al<sub>2</sub>O<sub>3</sub>-13wt% TiO<sub>2</sub> feedstock powder (Nanox S2613S). It is possible to confirm that this feedstock was formed by the agglomeration, via spray-drying, of individual Al<sub>2</sub>O<sub>3</sub> and TiO<sub>2</sub> particles. Among the feedstock powders employed in this study, this one exhibits the highest degree of homogeneity (level of mixing of the Al<sub>2</sub>O<sub>3</sub> and TiO<sub>2</sub> particles) (Fig. 2a). The particle of Fig. 2a, observed at higher SEM magnifications using secondary electrons (SE) is shown in Fig. 2b. It can be seen that the microscopic spray-dried material is formed by the agglomeration of individual particles with diameters varying from approximately 15 nm to 300 nm. Nanostructured material is normally defined as exhibiting grain/particle sizes that are less than 100 nm in at least one dimension, therefore this is not strictly a nanostructured feedstock. The expression “bimodal powder” or “hybrid powder”, indicating the presence of nanostructured (i.e., <100 nm) and submicron particles (i.e., 100 nm-500 nm), is more scientifically rigorous.

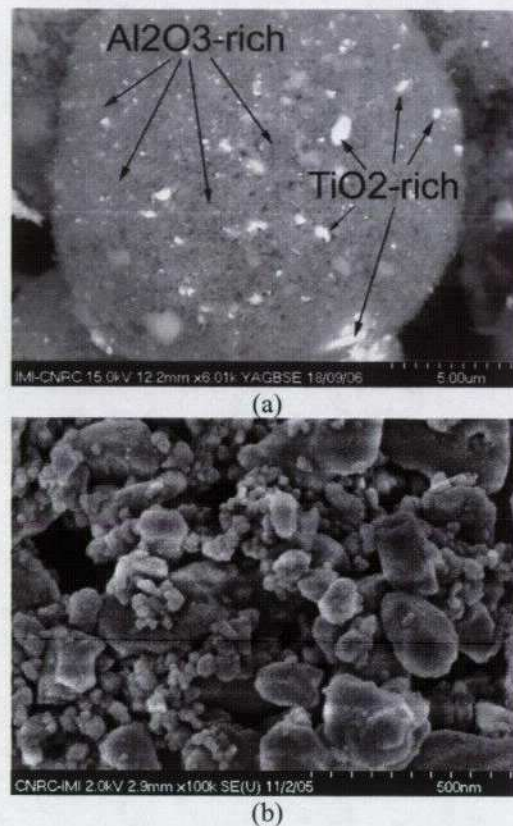


Figure 2: (a) SEM picture (BSE) of the Al<sub>2</sub>O<sub>3</sub>-13wt% TiO<sub>2</sub> powder Nanox S2613S. (b) Particle of (a) observed at higher magnification (SE).

Therefore, the term “hybrid powder” and “hybrid coating” will be used in this article to describe the Nanox S2613S Al<sub>2</sub>O<sub>3</sub>-13wt% TiO<sub>2</sub> feedstock powder and its coatings, respectively. Finally, it is important to point out that the hybrid particles are porous, which will probably influence the in-flight particle characteristics, as shown in the next section.

The second conventional Al<sub>2</sub>O<sub>3</sub>-13wt% TiO<sub>2</sub> feedstock powder (Metco 130) is clad, i.e., it was made via the cladding of fused and crushed Al<sub>2</sub>O<sub>3</sub> particles by a thin layer of submicron TiO<sub>2</sub> particles. Detailed SEM pictures of this powder can be found in different references [1, 2].

#### In-Flight Particle Characteristics

The results of average T & V for the plasma sprayed powders were found to be in the range of (i) 2356-2700°C and 261-367 m/s for the Metco 130 powder and (ii) 2479-2687°C and 268-388 m/s for the Nanox S2613S (APS cut) powder, respectively. This wide range of average particle T & V probably guaranteed that different coating microstructures were formed during thermal spraying, i.e., it may be stated that is in general a fair representation of Al<sub>2</sub>O<sub>3</sub>-13wt% TiO<sub>2</sub> coatings that can be engineered via APS.

The average and standard deviation of the T & V for the HVOF-sprayed particle distributions were found to be (i)  $2133 \pm 138^\circ\text{C}$  and  $863 \pm 109 \text{ m/s}$  for the Amperit 744.0 (HVOF cut) powder and (ii)  $2382 \pm 278^\circ\text{C}$  and  $985 \pm 95 \text{ m/s}$  for the Nanox S2613S (HVOF cut) powder. The two types of HVOF-sprayed coatings were sprayed with the same set of spray parameters; however, the T & V values achieved by the hybrid powder were approximately 10% higher than those achieved by the conventional powder. It must be pointed out that the HVOF parameter set used to spray both powders corresponded to the maximum propylene flow that could be fed into the DJ2700-hybrid torch at a constant rate. Therefore, the difference of approximately 10% in T & V values between the two groups of feedstock particles was not intentionally produced. It is also important to point out that HVOF spraying of ceramic oxides is carried out at the limit of the HVOF systems, due to their low flame temperatures (typically below  $3000^\circ\text{C}$ ) and the high melting point of ceramic materials.

There is one hypothesis to explain this difference of T & V values observed when using the same spray parameters for both powders. The conventional particles are dense (Fig. 1), therefore they should conduct heat better than the hybrid particles (Fig. 2), which are also porous. In addition, the hybrid particles have larger surface areas when compared to the conventional particles. Therefore, the large surface area probably translates into a better capacity to absorb heat from the HVOF flame. The porous structure of the hybrid powder could act as a thermal barrier, consequently the heat absorbed at the particle surface may propagate at lower rates towards the particle inner core when compared to those of the conventional fused and crushed fully dense particles. As a general consequence, due to the higher surface area and lower thermal conductivity, the hybrid particles would have a tendency to exhibit higher surface temperatures, which are the temperatures measured by the pyrometric system of the DPV 2000. The higher particle velocities attained by the hybrid particles may be related to their lower densities (porous structure), i.e., they are lighter than the fully dense particles.

It is important to point out that this phenomenon of higher particle T & V values measured for the HVOF-sprayed hybrid particles was also observed during plasma spraying. When the same plasma spray parameters were used to spray the hybrid (Nanox S2613S) and conventional (Metco 130) powders, the T & V values measured for the hybrid powders were higher than those measured for the conventional (clad) powder. As the clad powder is fully dense, the same hypothesis can be used here to explain this difference of T & V values. However, as plasma spraying of ceramics does not have the same constraints of HVOF, higher plasma currents or  $\text{H}_2$  flows (or both) were used for spraying the conventional feedstock (Metco 130) in order to attain T & V values similar to those measured for the hybrid particles.

### Abrasion Wear Resistance

The abrasion wear resistance values of the coatings produced for this study were ranked in terms of volume loss, i.e., the lower the volume loss, the higher the wear resistance (Fig. 3).

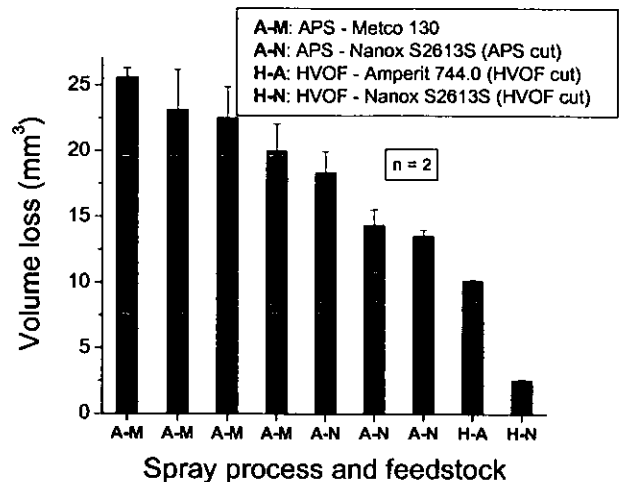


Figure 3: Volume loss versus for each combination of spray process and feedstock.

From Fig. 3 it is possible to observe that among the APS coatings, the four conventional ones exhibited lower wear resistance (i.e., higher volume loss) than the three hybrid coatings. However, the HVOF-sprayed conventional coating outperformed the best APS hybrid coating. On the other hand, the best performing anti-wear coating of all was the HVOF-sprayed hybrid coating. From the optimized ASP conventional coating to the HVOF-sprayed hybrid coating, there was a reduction in volume loss of 87%, or an improvement of 8 times in wear performance.

The explanation for the enhanced wear behavior of APS coatings produced from spray-dried (nanostructured)  $\text{Al}_2\text{O}_3$ -13wt%  $\text{TiO}_2$  powders when compared to conventional coatings (clad powder - Metco 130) has been hypothesized by different authors [1, 2]. Gell et al. [1] hypothesized (with some level of experimental evidence) that semi-molten nanostructured feedstock particles embedded in the coating microstructure would act as crack arresters, thereby increasing the toughness of the coatings. Ahn et al. [2] proposed another hypothesis (with some level of experimental evidence). The melting point of pure  $\text{Al}_2\text{O}_3$  is  $\sim 2050^\circ\text{C}$ , whereas, the melting point of  $\text{Al}_2\text{O}_3$ -13wt%  $\text{TiO}_2$  is  $\sim 1940^\circ\text{C}$ . Ahn et al. observed that the spray-dried nanoagglomerates exhibited a homogeneous mixing of  $\text{Al}_2\text{O}_3$  and  $\text{TiO}_2$  particles (such as that of Fig. 2), which in turn would tend to lower the melting point of each agglomerate (by the addition of  $\text{TiO}_2$  to  $\text{Al}_2\text{O}_3$ ), lowering particle viscosity, thereby improving the interlamellar contact (i.e., coating toughness) at impact during spraying [2]. Due to the existence of these hypotheses for APS coatings, this work will

concentrate in the development of a hypothesis for explaining the enhanced wear behavior of the HVOF-sprayed hybrid coatings, as shown in the next sections.

#### Hardness, Porosity and Crack Propagation Resistance

Table 3 shows the porosity and Vickers microhardness values obtained for the coatings involved in this study. It is evident that the hardness values alone do not provide enough information to explain the enhanced wear performance of the HVOF-sprayed hybrid coating.

Table 3: Porosity and Vickers microhardness values.

Coating	P (%)	HV (300 g)
APS Metco 130	1.9 – 4.7	970 - 1093
APS Nanox S2613S	2.6 – 4.4	776 - 1057
HVOF Amperit 744.0	2.2 ± 0.3	832 ± 41
HVOF Nanox S2613S	<1	808 ± 40

The crack propagation resistance values of the two HVOF-sprayed coatings were measured. The values were  $30.5 \pm 3.3$  MPam<sup>1/2</sup> and  $25.5 \pm 0.7$  MPam<sup>1/2</sup> for the hybrid (Nanox S2613S) and conventional coatings (Amperit 744.0), respectively (the Vickers microhardness (300 g) and crack propagation resistance of the optimized APS Metco 130 coating were  $1080 \pm 58$  and  $14.0 \pm 2.5$  MPam<sup>1/2</sup>). Therefore, in relative terms, the HVOF-sprayed hybrid coating was tougher than the conventional one. This difference in crack propagation behavior under Vickers indentation is shown in Figs. 4 and 5. From these pictures it is observed that the hybrid coating exhibits a more homogeneous microstructure than that of the conventional coating. Due to the nature of the conventional feedstock Amperit 744.0 (Fig. 1), it seems logical to assume that Al<sub>2</sub>O<sub>3</sub> and TiO<sub>2</sub> particles will not be homogeneously mixed in the coating microstructure. Therefore the white-colored and dark-colored regions in this SEM (SE) image (Fig. 4) probably represent Al<sub>2</sub>O<sub>3</sub> and TiO<sub>2</sub>-rich regions, respectively. As TiO<sub>2</sub> has a lower mechanical strength than Al<sub>2</sub>O<sub>3</sub>, the TiO<sub>2</sub>-rich lamellar zones will probably exhibit lower interlamellar strength, thereby lowering the coating toughness, as seen in Fig. 4.

On the other hand, the HVOF-sprayed hybrid coating (Fig. 5) exhibits a more homogeneously mixed microstructure, which is probably the result of the intimate Al<sub>2</sub>O<sub>3</sub> and TiO<sub>2</sub> particle mixing of the agglomerates (Fig. 2a). Based on the hypothesis proposed by Ahn et al. [2], this intimate Al<sub>2</sub>O<sub>3</sub> and TiO<sub>2</sub> particle mixing would result in lowering the melting point of each agglomerate (TiO<sub>2</sub> addition to Al<sub>2</sub>O<sub>3</sub>) during thermal spraying, which would lower the viscosity of the particles. The lower viscosity would provide the splats improved wetting and interlamellar strength, thereby increasing coating toughness, as seen in Fig. 5.

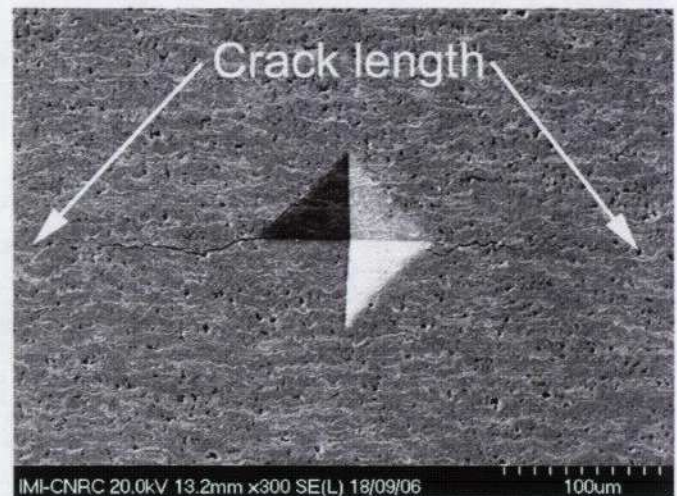


Figure 4: Crack propagation under Vickers indentation for the HVOF-sprayed conventional (Amperit 744.0) coating.

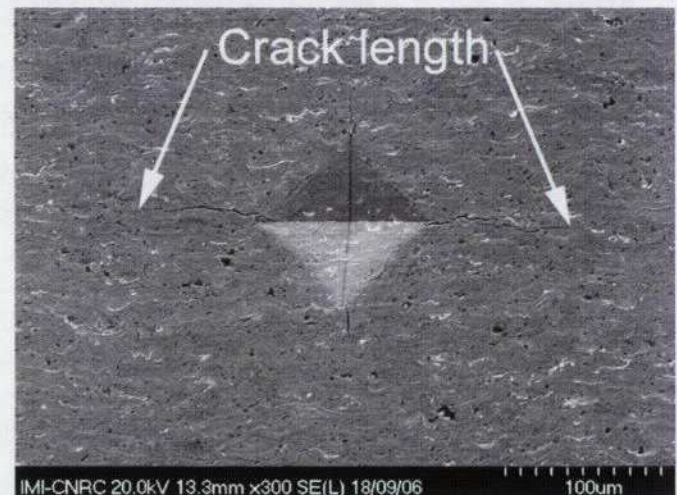
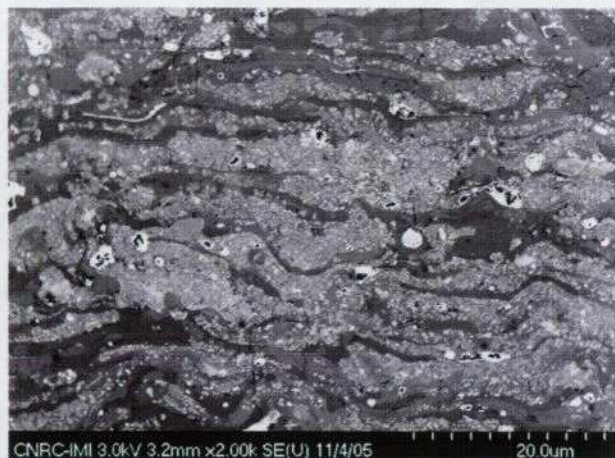


Figure 5: Crack propagation under Vickers indentation for the HVOF-sprayed hybrid (Nanox S2613S) coating.

It is important to point out that not all hybrid particles were fully molten during HVOF spraying. Figure 6 shows an SEM picture (SE) of the HVOF-sprayed hybrid (Nanox S2613S) coating of Fig. 5 taken at higher magnifications. It is possible to observe zones of finely dispersed material (similar to that found in HVOF-sprayed WC-Co coatings) spread throughout the coating microstructure (Fig. 6a). By comparing these zones of finely dispersed material to the morphology of the Nanox S2613S hybrid powder (Fig. 2), it can be suggested that they probably correspond to semi-molten hybrid particles that were embedded in the coating microstructure during HVOF spraying. It is also interesting to follow the path of the Vickers indentation cracks (such as that of Fig. 5) at higher magnifications (Fig. 6b). It was observed that the crack arrested after passing through a semi-molten zone. It was also observed that the non-molten nano and submicron particles

diverted the crack, producing a more tortuous crack path helping to consume energy. This phenomenon is similar to that observed by Gell et al. for the same material [1].



(a)



(b)

Figure 6: (a) SEM picture of the HVOF-sprayed Nanox S2613S coating of Fig. 5 taken at higher magnifications – zones of finely dispersed material containing semi-molten hybrid particles. (b) Vickers indentation crack arrested after being diverted by passing through a semi-molten hybrid particle.

The percentage of semi-molten hybrid particles embedded in the coating microstructure of the HVOF-sprayed coating was measured via image analysis, based on ten SEM pictures taken using the same characteristics and magnification of Fig. 6a, and was found to be  $52 \pm 6\%$ .

### Conclusions

During this work, three types of  $\text{Al}_2\text{O}_3$ -13wt%  $\text{TiO}_2$  powders were employed in this study. One designated as “hybrid”, which was formed by agglomeration via the spray-drying of

nanostructured and submicron particles (15-300 nm), and two conventional (blended and clad). The conclusions are the following:

All four APS coatings produced from the conventional (clad) powder exhibited poorer wear resistance when compared to the three APS coatings produced from the hybrid powder.

When the optimized APS conventional (clad) coating is compared to the HVOF-sprayed hybrid coating, a reduction in volume loss of 87%, or an improvement of 8 times in wear performance is observed for the HVOF-sprayed hybrid material. The percentage of semi-molten particles embedded in the microstructure of the HVOF-sprayed hybrid coating was found to be  $52 \pm 6\%$ .

It is hypothesized that two mechanisms are acting together for producing the enhanced toughness and wear performance for the HVOF-sprayed hybrid coating. (i) The high degree of  $\text{Al}_2\text{O}_3$  and  $\text{TiO}_2$  mixing in each hybrid agglomerate probably lowers its melting point (addition of  $\text{TiO}_2$  to  $\text{Al}_2\text{O}_3$ ) producing a lowering of the particle viscosity (at least at the surface) and improving the interlamellar contact at impact during HVOF spraying. (ii) Cracks tend to lose their energy by being diverted when passing through the semi-molten hybrid particles embedded in the coating microstructure.

### References

1. M. Gell, E.H. Jordan, Y.H. Sohn, D. Goberman, L. Shaw, and T.D. Xiao, Development and Implementation of Plasma Sprayed Nanostructured Ceramic Coatings, *Surf. Coat. Technol.*, Vol 146-147, 2001, p 48-54
2. J. Ahn, B. Hwang, E.P. Song, S. Lee, and N.J. Kim, Correlation of Microstructure and Wear Resistance of  $\text{Al}_2\text{O}_3$ - $\text{TiO}_2$  Coatings Plasma Sprayed with Nanopowders, *Metall. Mater. Trans. A*, Vol 37A, June, 2006, p 1851-1861
3. R.S. Lima and B.R. Marple, From APS to HVOF Spraying of Conventional and Nanostructured Titania Feedstock Powders: a Study on the Enhancement of the Mechanical Properties, *Surf. Coat. Technol.*, Vol 200, 2000, p 3428-3437
4. G.R. Anstis, P. Chantikul, B.R. Lawn, and D.B. Marshall, A Critical Evaluation of Indentation Techniques for Measuring Fracture Toughness: I. Direct Crack Measurements, *J. Am. Ceram. Soc.*, Vol 64 (No. 9), 1981, p 1073-1082
5. “Standard Test Method for Measuring Abrasion Using the Dry Sand/Rubber Wheel Apparatus,” G65-00, *Annual Book of ASTM Standards*, ASTM 2000, p 1-12
6. R.S. Lima and B.R. Marple, “Optimized HVOF Titania Coatings,” *J. Therm. Spray Technol.*, 2003, 12(3), p 360-68